Available online at www.sciencedirect.com

SCIENCE DIRECT

Developmental Biology 279 (2005) 86–98

DEVELOPMENTAL BIOLOGY

www.elsevier.com/locate/ydbio

# Normal newt limb regeneration requires matrix metalloproteinase function

Vladimir Vinarsky[a,b,c,d], Donald L. Atkinson[a], Tamara J. Stevenson[a], Mark T. Keating[c,d], Shannon J. Odelberg[a,b,*]

[a]*Division of Cardiology, Department of Internal Medicine, University of Utah, Salt Lake City, UT 84132, USA*
[b]*Department of Neurobiology and Anatomy, University of Utah, Salt Lake City, UT 84132, USA*
[c]*Department of Cell Biology, Howard Hughes Medical Institute, Harvard Medical School, Boston, MA 02115, USA*
[d]*Department of Cardiology, Children's Hospital, Boston, MA 02115, USA*

Received for publication 12 July 2004, revised 17 November 2004, accepted 3 December 2004
Available online 13 January 2005

**Abstract**

Newts regenerate lost limbs through a complex process involving dedifferentiation, migration, proliferation, and redifferentiation of cells proximal to the amputation plane. To identify the genes controlling these cellular events, we performed a differential display analysis between regenerating and nonregenerating limbs from the newt *Notophthalmus viridescens*. This analysis, coupled with a direct cloning approach, identified a previously unknown *Notophthalmus* collagenase gene (*nCol*) and three known matrix metalloproteinase (MMP) genes, *MMP3/10a*, *MMP3/10b*, and *MMP9*, all of which are upregulated within hours of limb amputation. *MMP3/10b* exhibits the highest and most ubiquitous expression and appears to account for the majority of the proteolytic activity in the limb as measured by gel zymography. By testing purified recombinant MMP proteins against potential substrates, we show that nCol is a true collagenase, MMP9 is a gelatinase, MMP3/10a is a stromelysin, and MMP3/10b has an unusually broad substrate profile, acting both as a stromelysin and noncanonical collagenase. Exposure of regenerating limbs to the synthetic MMP inhibitor GM6001 produces either dwarfed, malformed limb regenerates or limb stumps with distal scars. These data suggest that MMPs are required for normal newt limb regeneration and that MMPs function, in part, to prevent scar formation during the regenerative process.


*Keywords:* Limb regeneration; Matrix metalloproteinase; *nCol*; *MMP3/10b*; *MMP3/10a*; *MMP9*; Blastema; *Notophthalmus viridescens*; Newt

## Introduction

Newts and other salamanders have the remarkable ability to regenerate their limbs, tails, jaws, spinal cords, lenses, retinas, and heart ventricles (Brockes and Kumar, 2002; Butler and Ward, 1967). This regenerative ability is dependent upon an unusual degree of cellular plasticity near the site of injury. Following limb amputation, epithelial cells proximal to the amputation plane convert to a migratory form and cover the wound completely within 24 h, while internal limb cells begin to dedifferentiate to form a mass of proliferating progenitor cells known as the regeneration blastema (Bodemer and Everett, 1959; Chalkley, 1954; Hay and Fischman, 1961). The newly-formed wound epithelium (WE) is required for the growth of the regenerating salamander limb (Mescher, 1976; Thornton, 1957) and its later derivative, the apical epithelial cap (AEC), can even promote supernumerary limb formation when transplanted to a more proximal region of an existing regeneration blastema (Thornton and Thornton, 1965). In the newt *Notophthalmus viridescens*, dedifferentiation begins in the first week following limb loss and the blastemal stage lasts through the third or fourth week of regeneration. Complete replacement of the limb occurs within 5–7 weeks (Wallace, 1981).

Although previous studies have identified many of the early cellular events leading to the formation of the WE/

* Corresponding author. Division of Cardiology, Department of Internal Medicine, University of Utah Health Sciences Center, Wintrobe Building, Room 667, 26 North 1900 East, Salt Lake City, UT 84132, USA. Fax: +1 801 581 8552.
*E-mail address:* odelberg@howard.genetics.utah.edu (S.J. Odelberg).

0012-1606/$ - see front matter © 2004 Elsevier Inc. All rights reserved.
doi:10.1016/j.ydbio.2004.12.003

AEC and the regeneration blastema, little is known about the molecular mechanisms that control these processes. Candidate genes upregulated during the early phases of limb regeneration include matrix metalloproteinases (MMPs). MMPs were discovered in 1962 as proteases capable of digesting the collagen present in the tail skin, gills, and intestines of bullfrog tadpoles (Gross and Lapiere, 1962). It was soon demonstrated that a similar collagenolytic activity was also present in the regenerating limbs of newts but absent in nonregenerating limbs (Grillo et al., 1968). Over the past four decades, more than 25 vertebrate MMPs have been identified and classified into groups according to their protein structure and substrate specificity. These groups include collagenases (MMP1, MMP8, MMP13, and MMP18), gelatinases (MMP2 and MMP9), stromelysins (MMP3, MMP10, and MMP11), and the membrane-type MMPs (MMP14, MMP15, MMP16, MMP17, MMP24, and MMP25) (Sternlicht and Werb, 2001). Most MMPs are secreted in a latent form and must be activated by cleavage of an N-terminal propeptide domain. Activation can occur through the actions of other proteases, chaotropic agents, or organomercuric compounds such as 4-aminophenylmercuric acetate (APMA). Although MMP activity is known to increase during salamander limb regeneration (Grillo et al., 1968; Park and Kim, 1999; Yang and Bryant, 1994) and some of the MMP genes responsible for this activity have been cloned (Kato et al., 2003; Miyazaki et al., 1996; Yang et al., 1999), previous studies have not established whether these proteases are required for the regenerative process nor have they investigated the biochemical function of salamander MMPs through substrate analysis.

We have performed a differential display analysis between regenerating and nonregenerating limbs from *N. viridescens* to identify genes that might play important roles in the initial stages of regeneration. This screen, coupled with a direct cloning approach, has identified a new *Notophthalmus* collagenase gene (*nCol*) and three MMP genes previously cloned in other species, *MMP3/10a*, *MMP3/10b*, and *MMP9*, all of which are upregulated within hours of limb amputation. We have determined the temporal and spatial expression patterns for each of these MMP genes, have characterized the substrate specificities of their recombinant proteins, and assessed their in vivo function by performing MMP inhibitor studies during the regenerative process. We conclude that MMPs are required for normal limb regeneration and that they apparently function, in part, to prevent scar formation during the regenerative process.

## Materials and methods

### *Newt limb amputations*

All procedures involving newts were approved by the University of Utah Institutional Animal Care and Use Committee. Limb amputations were performed as previously described (McGann et al., 2001), except that the bone was not trimmed following amputation. The limbs were reamputated 1.5–2.5 mm proximal to the distal tip of the regenerating limb.

### *Differential display analysis*

Differential display was performed according to the manufacturer's instructions (GenHunter) using 80 random primers and three oligo-dT primers containing either a dA, dG, or dC on their 3′-ends. Total RNA from regenerating (days 1, 3, and 5) and intact (day 0) newt limbs was isolated for analysis. Differentially-displayed cDNA fragments were excised from the polyacrylamide gel, eluted, and reamplified. The reamplified cDNAs were TA cloned into pBluescript II, and multiple clones were selected, restriction mapped, and sequenced.

### *Northern blot analysis*

Northern blot analysis was performed on RNA extracted from regenerating newt limbs at 0, 18, 24, and 72 h and 5, 10, 15, 20, 25, 30, 35, and 40 days postamputation. Total RNA (2–10 μg) was separated on 1% denaturing agarose gels in 1× MOPS buffer (20 mM MOPS, 5 mM sodium acetate, 1 mM EDTA, pH 7) containing 0.5 M formaldehyde, transferred to Hybond $N^+$ nylon membrane (Amersham Pharmacia), and stained with methylene blue to assess transfer efficiency and RNA loading equivalency between lanes. The blots were hybridized with [$^{32}$P]-α-dCTP-labeled probes and phosphorimaging was performed using a Storm 860 (Molecular Dynamics). Signals were normalized using densitometric analysis of the methylene blue-stained 28S and 18S rRNAs.

### *RLM-RACE and sequencing of full-length cDNAs*

cDNAs containing the full-length open reading frames for *MMP3/10a*, *MMP3/10b*, and *MMP9* were obtained by RNA ligase-mediated-rapid amplification of cDNA ends (RLM-RACE) according to the manufacturer's instructions (Ambion) with the following minor modifications. Following linker attachment to the decapped 5′-ends of the mRNAs, oligo-dT 3′-primers and Superscript II were used for first strand cDNA synthesis. Nested PCR was then performed using *Pfu*Ultra DNA polymerase (Stratagene) or Advantage Taq (Clontech) in the presence of 5′-linker primers and 3′-specific gene primers, which were constructed based on the sequences obtained from differential display products. The amplification products were gel purified, TA cloned into pBluescript II, and sequenced. *nCol* was cloned in two steps. First, the 5′-end of the cDNA, which contained all but the last 24 bp of the open reading frame, was cloned as described above. The remaining 24 bp, which included the stop codon, was added by PCR amplification of the 5′-end of the cDNA using a 3′-primer

that contained a tail with the missing 24 nucleotides and a *Not*I restriction site for directional cloning. The 5′-primer contained the restriction site *Hin*dIII for directional cloning. The amplification product was gel purified, directionally cloned into pBluescript II, and sequenced. Comparisons of predicted amino acid sequences were done using either the BLAST 2 sequences (Tatusova and Madden, 1999) or Clustal W programs (Thompson et al., 1994).

Primer sequences used to clone the above genes are shown below. The *Bam*HI, *Hin*dIII, and *Not*I sites, which were used for some of the cloning procedures, are underlined.

Ambion 5′-RACE primers:

5′-RACE outer primer, 5′-GCTGATGGCGATGAATGAACACTG-3′;
5′-RACE inner primer 5′-CGCGGATCCGAACACTGCGTTTGCTGG-CTTTGATG-3′;

Specific 3′-MMP primers:

MMP3/10a 3′-outer primer, 5′-AAACATACACTTAATAAGTATTTTGTT-CTG 3′;
MMP3/10a 3′-inner primer, 5′-TAAACCAAGTTTTCAGCATTGAATTC-TAG-3′;
MMP3/10b 3′-outer primer, 5′-CAAGCTGAATTTAGTGCTCTTTCAAC-3′
MMP3/10b 3′-inner primer, 5′-AGTAAACTTTTATCAACAACT-GAACCA-3′
MMP9 3′-outer primer, 5′- CTGAAAACACACACATCCTAACCTTG-3′;
MMP9 3′-inner primer, 5′-TCAAATCTTGTGGCACTTGCGCCAGG-3′;
nCol 3′-outer primer, 5′-GAAAGACCATGTGTGCCGCTAGTAAGCAT-AG-3′;
nCol 3′-inner primer, 5′-GCTGTTGTTCCTCAAGACCCGCAT-CACTCTC-3′;
nCol 5′-full-length primer, 5′-CACACACACAAAGCTTAAAAGGGAT-CAGAGAAACTTGTCCAC-3′;
nCol 3′-full-length primer, 5′-CACACACACAGCGGCCGCGGGCTT-TATGCTTCTTGACATCCCAACCAGCTGTTGTTCCTCAAGACCC-GCATCAC-3′;

*RNA in situ hybridization*

One-, five-, and fifteen-day limb regenerates were amputated at the shoulder and the limbs were fixed overnight in Carnoy's fixative (60% ethanol, 30% chloroform, 10% glacial acetic acid). Following 24 h of decalcification in Morse's solution (387 mM sodium citrate, 22.5% formic acid), the limbs were washed with PBS and dehydrated through a series of ethanol/PBS washes with increasing ethanol concentration. The samples were equilibrated in Hemo-De, embedded in paraffin, and sectioned at 10 μm. The paraffin was removed with Hemo-De and the sections were rehydrated and postfixed with 4% paraformaldehyde in PBS for 15 min. Endogenous alkaline phosphatases were inhibited by treatment with 0.2 M HCl in PBS for 8 min. The tissues were digested with 5 μg/ml proteinase K for 15 min at 37°C, acetylated in 0.25% acetic anhydride (v/v) in 0.1 M triethanolamine for 15 min, and prehybridized for 30 min. Heat denatured digoxigenin-labeled riboprobe (250–500 ng/ml) in 50% formamide, 4× SSC, 1× Denhardt's solution, 500 μg/ml heat denatured herring sperm DNA, 200 μg/ml yeast RNA, and 10% PEG 6000 was added, and the samples were placed in a humidified chamber at 55°C overnight. The tissues were washed in buffer, treated with 40 μg/ml RNase A for 30 min at 37°C, and washed again. After blocking the tissues in 0.5% blocking reagent (Roche) for 30 min, the samples were treated for 1 h at room temperature with a 1/100 dilution of alkaline phosphatase-conjugated sheep anti-digoxigenin antibody (Roche) in 0.5% blocking reagent. The slides were washed and the sections were incubated 20 h in the dark at room temperature with NBT/BCIP substrate. The sections were mounted and observed using a light microscope.

*Purification of proteins by affinity chromatography*

cDNAs containing complete open reading frames (ORFs) were FLAG-tagged (amino acid sequence DYKDDDDK) on the 3′-end of their ORFs by PCR using *Pfu*Ultra DNA polymerase. The PCR products were directionally cloned into the mammalian expression vector pBK-CMV using either *Bam*HI and *Not*I or *Hin*dIII and *Not*I, depending upon the restriction sites present in the amplification primers. The MMP inserts were completely sequenced to ensure that no nucleotide substitutions had occurred during the amplification procedure and were then subcloned directionally into pCMV-SPORT6 (Invitrogen) using the *Sal*I and *Not*I sites in both vectors. The pCMV-SPORT6 clones were used for preparation of the recombinant MMP proteins, because they consistently produced higher protein yields than the pBK-CMV constructs. Each of the expression clones was separately transfected into human embryonic kidney 293H cells using Lipofectamine2000 (Invitrogen), and 100–200 ml of serum-free conditioned DMEM medium was collected from the transfected cells at 24–96 h post-transfection. FLAG-tagged proteins from the conditioned medium were purified by affinity chromatography according to the manufacturer's instructions using 300 μl of packed resin conjugated to anti-FLAG M2 antibody (Sigma). Concentrations of the affinity purified proteins were determined by comparison to a FLAG-tagged bovine alkaline phosphatase standard (Sigma) following Western blotting and chemiluminescence detection using the SuperSignal West Femto reagent (Pierce).

Primer sequences used for making the FLAG-tagged MMPs are shown below. Underlined sequences are either *Not*I or *Hin*dIII sites, italicized sequences are the complement of the stop codon, bold sequences are the complement of the FLAG-tag, uppercase, normal character sequences are gene specific, and lowercase sequences are nonspecific 5′protective sequences designed to enable cleavage at the restriction sites. nCol 5′-full-length primer (see above for sequence); nCol 3′-FLAG primer, 5′-cagtcaGCGGCCGC*T*-

*TA***CTTATCGTCGTCATCCTTGTAATC**TGCTTCTTGACATCCCAACCAGC-3′; MMP3/10b 5′-primer is the 5′-RACE inner primer (see above for sequence); MMP3/10b 3′-FLAG primer, 5′-cagtcaGCGGCCGC*TTATCA***CTTATCGTCGTCATCCTTGTAATC**ACAACTGAACCAGCTGTTTTTCGTCAG-3′; MMP3/10a 5′-primer is the 5′-RACE inner primer (see above for sequence); MMP3/10a 3′-FLAG primer, 5′-cagtcaGCGGCCGC*TTA***CTTATCGTCGTCATCCTTGTAATC**ACACCGTAACCAGCTGGTGTTCTTCAG-3′; MMP9 5′-primer, 5′-cacacacacaAAGCTTGAACACTGCGTTTGCTGGCTTTGATG-3′; MMP9 3′-FLAG primer, 5′-cagtcaGCGGCCGC*CTA***CTTATCGTCGTCATCCTTGTAATC**ATTCTCGGGGCAATTCAAGATGTCG-3′.

*Preparation of regeneration and intact limb extracts*

Regenerating newt limbs were collected at various time points following amputation, flash frozen in liquid nitrogen, and stored at −80°C for later extraction. Intact limbs were also collected and stored similarly. Regeneration and intact limb extracts were prepared as previously described (McGann et al., 2001) and stored at −80°C until needed.

*Zymography*

0.1% gelatin and 0.1% casein zymography gels were purchased from Bio-Rad. Purified FLAG-tagged nCol, MMP3/10b, MMP3/10a, and MMP9 (30 fmol to 1.5 pmol) or regeneration and intact limb extracts (15–25 μg) were separated by electrophoresis for 90 min at 100 V through gelatin and casein zymography gels. The MMPs were renatured in three washes of 2.5% Triton X-100 (10 min each), followed by an 18–24 h incubation in development buffer (50 mM Tris–HCl, pH 7.6, 10 mM $CaCl_2$, 50 mM NaCl, 0.05% Brij-35). Gels were stained with Coomassie blue R250 for ~1 h and then destained in multiple changes of a 40% methanol/10% acetic acid solution until clear bands were visible (2–3 h).

*DQ- and BODIPY-substrate assays*

DQ-gelatin, DQ-collagen I, DQ-collagen IV (100 μg/ml), and BODIPY FL-casein (10 μg/ml) substrates (Molecular Probes) were mixed with 1.5 pmol of purified nCol, MMP3/10b, MMP3/10a, or MMP9 in the presence of 1 mM APMA and enzyme activation buffer (50 mM Tris–HCl, pH 7.6, 150 mM NaCl, 5 mM $CaCl_2$, 1 μM $ZnSO_4$, and 0.05% Brij-35). Controls consisted of mixtures of purified MMP protein and substrate without APMA activation and mixtures of AMPA and substrate alone. For the inhibitor assays, 2 μM GM6001 was mixed with the individual MMPs in 1 mM APMA. Fluorescence signals were measured on a Perkin-Elmer Fusion α microplate reader at various time points up to 3 days.

*Rat tail type I collagen assay*

Native rat tail type I collagen (0.5 mg/ml) was mixed with either APMA-preactivated MMP proteins (5–14 nM) or with the purified proMMP proteins (5–14 nM) plus 1 mM APMA in enzyme activation buffer (see above) and incubated for 6–24 h at 25°C or 30°C. Following the incubation period, one quarter volume of 4× reducing SDS loading buffer was added to the reactions and the samples were heated to 95°C for 3 min to denature the proteins. The samples were separated by SDS–PAGE at 180 V until the bromophenol blue ran off the bottom of the gel and then stained with Gelcode Blue (Pierce). Controls included mixtures of either unactivated proMMP and rat tail type I collagen or APMA plus rat tail type I collagen.

*In vivo GM6001 studies*

Following limb amputation and a 1 h recovery period on ice, newts were housed in one of the following solutions: (1) 50 μM GM6001/1% DMSO in dechlorinated tap water; (2) 1% DMSO in dechlorinated tap water; or (3) dechlorinated tap water. Fresh solutions were either prepared every 4 days, or alternatively, the solutions were sterile filtered with a 0.2 μm filter every 4 days and entirely replaced every 8 days. The inhibitory activity of the used GM6001 solution was confirmed by its ability to inhibit MMPs during gel zymography. Following 60 days of regeneration, the limbs were amputated at the shoulder, fixed in Carnoy's fixative overnight, decalcified for 1 h in a 2 M HCl/PBS/0.5% Triton X-100 solution, and neutralized in 100 mM sodium borate (pH 8.4) for 5 min. The limbs were washed twice in PBS, dehydrated, embedded in paraffin, and sectioned at 10 μm. The sections were stained with hematoxylin and eosin, and photographs and bone measurements were taken using a Zeiss Axiocam and Axiovision software. The length of the regenerated humerus was measured from the distal end of the ossified bone to the end of the cartilaginous humerus. Length and width measurements represent maximum values.

## Results

*Cloning of N. viridescens MMP genes*

Differential display analyses between 1-, 3-, and 5-day limb regenerates and intact limbs identified three MMP genes that were upregulated during the early stages of limb regeneration. Full-length cDNAs were generated for each of these genes using RLM-RACE. Sequence analysis revealed that one of the genes, *nCol*, was a previously unknown newt collagenase with a predicted amino acid sequence sharing 64%/78% identity/similarity (I/S) with

*Xenopus* MMP18 and 57%/73%, 54%/72%, and 54%/66% I/S with the human collagenases MMP1, MMP8, and MMP13, respectively (Fig. 1A). From sequence analysis alone, it is unclear which, if any, of the known collagenases is orthologous to this newt MMP. Furthermore, biochemical functional analyses (see below) demonstrate that nCol has a slightly different substrate profile than its closest known homolog, *Xenopus* MMP18, suggesting that these two proteases might not be orthologs. Two of the upregulated MMP genes are orthologs of

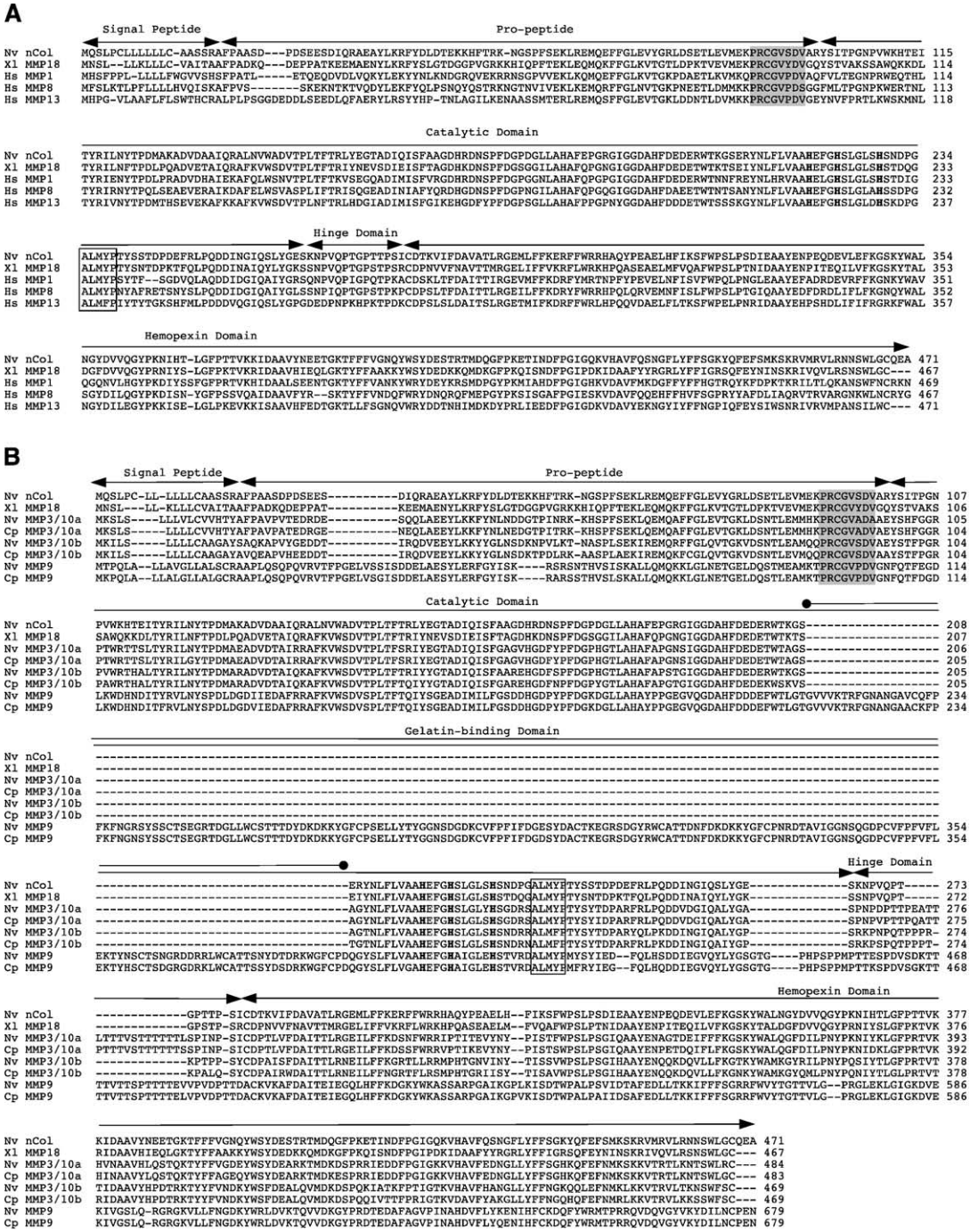


Fig. 1. Deduced amino acid sequences of *N. viridescens* (Nv) MMPs and comparison to MMPs from other species. (A) The nCol sequence is compared to *X. laevis* (Xl) MMP18 and the human (Hs) collagenases MMP1, MMP8, and MMP13. (B) The four *N. viridescens* MMPs are compared to each other and the most closely related MMPs from either *X. laevis* or *C. pyrrhogaster* (Cp). The major domains are delineated by the double arrowed lines. The histidine residues that bind zinc are in bold. The shaded boxes highlight the cysteine switch region involved in maintaining MMP latency, while the white boxes identify the conserved Met turn sequence that lies downstream of the zinc-binding motif. GenBank accession numbers for the sequences reported here are AY857753 (*nCol*), AY857751 (MMP3/10a), AY857754 (MMP3/10b), and AY857752 (MMP9).

*MMP9* and *MMP3/10a* with predicted amino acid sequences exhibiting 95%/98% and 94%/95% I/S, respectively, to the corresponding genes from *C. pyrrhogaster* (Fig. 1B).

A full-length *N. viridescens MMP3/10b* cDNA was cloned by RLM-RACE using primers based on *C. pyrrhogaster* sequences and RNA collected from early limb regenerates. We confirmed the 3′-end of the RLM-RACE sequence, which contained the original *C. pyrrhogaster* primer sequence, by subsequent 3′-RACE and sequencing. The predicted amino acid sequence for *N. viridescens* MMP3/10b revealed 87%/93% I/S to the corresponding *C. pyrrhogaster* sequence (Fig. 1B).

### *Temporal RNA expression patterns of MMP genes during limb regeneration*

Temporal RNA expression patterns were obtained for each of the MMP genes during the first 40 days of newt limb regeneration. Northern blot analyses demonstrated that *nCol* and *MMP9* followed bimodal expression patterns (Fig. 2A). Both genes reached maximum expression levels 24 h postamputation (*nCol*, 11-fold upregulation; *MMP9*, 10-fold), reduced their expression levels by day 3, and then reached a second peak at 10–15 days postamputation (9- and 7-fold, respectively). *MMP3/10a* and *MMP3/10b* were similarly upregulated within hours of limb amputation, reaching maximum expression levels at 18–24 h (19- and 21-fold, respectively). Following this initial burst, RNA expression for *MMP3/10b* returned to preamputation levels by regeneration day 30, while *MMP3/10a* expression rapidly declined and returned to preamputation levels by days 10–15. The degree of upregulation was determined by phosphorimaging analysis and normalization to the 28S and 18S rRNA bands following methylene blue staining (see Materials and methods).

### *Temporal MMP proteolytic activity during newt limb regeneration*

Proteolytic analyses of regenerating limb extracts using casein and gelatin zymography revealed that the activities of certain proteases increase markedly during the early stages of limb regeneration (Fig. 2B). These proteases are inhibited by the MMP inhibitor GM6001 (see below) and 5 mM EDTA, but not by 1 mM phenylmethylsulfonyl fluoride (PMSF) (data not shown), confirming that they are bona fide MMPs. Both casein and gelatin zymography revealed a prominent ~20 kDa MMP whose activity increased within 4–6 h of limb amputation and reached its peak by 24 h. The activity of the 20 kDa MMP remained high through regeneration day 20 and returned to preamputation levels by day 40. Several other caseinolytic MMPs, ranging in size from 25 to 60 kDa, exhibited increased activity during the early stages of limb regeneration. In addition to the prominent 20 kDa MMP, gelatin zymography revealed the presence of three other MMPs with molecular weights of 60, 70, and 85 kDa. The 85 kDa MMP exhibited a bimodal activity pattern with peaks at 18–24 h and 10–20 days postamputation. The activities of the 60 and 70 kDa MMPs remained low through regeneration day 10, then increased slightly by day 15, and remained marginally elevated through day 40.

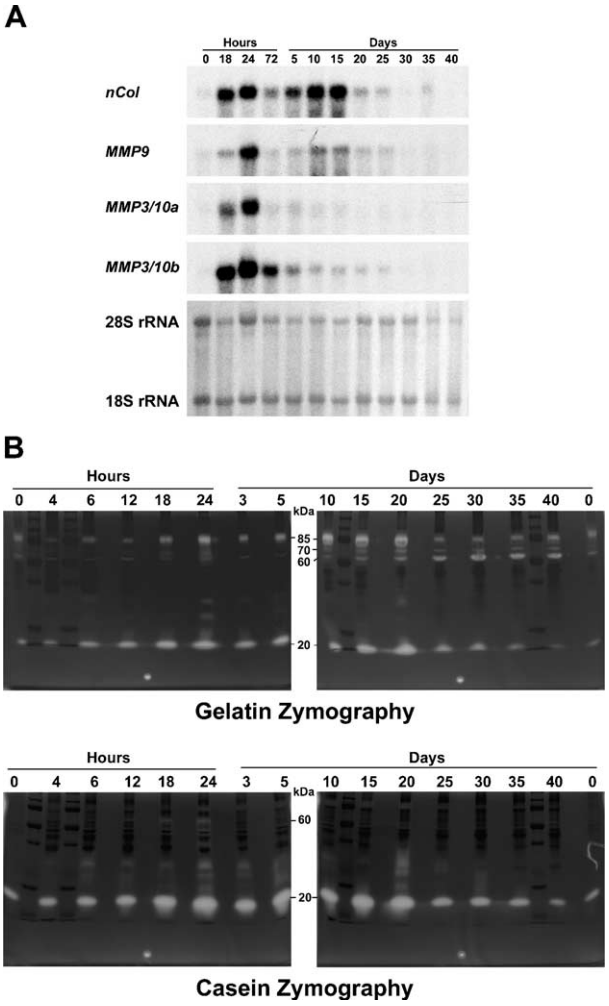


Fig. 2. Temporal RNA expression and proteolytic activity of MMPs during newt limb regeneration. (A) Northern blot analyses of *nCol*, MMP9, MMP3/10a, and MMP3/10b during the first 40 days of limb regeneration. Each lane contained 2 μg of total RNA. Membranes were stained with methylene blue to assess loading equivalency and transfer efficiency and to allow for normalization of RNA between lanes. An example of a membrane stained with methylene blue is shown in the bottom panel. (B) Gelatin and casein zymography were used to assess MMP activity over the first 40 days of limb regeneration. Each lane contained 15 μg of limb extract. Numbers above the lanes refer to hours or days postamputation.

It is possible to tentatively assign most of the MMPs identified by zymography to MMPs known to be upregulated during newt limb regeneration based on size, substrate specificity, and a comparison of temporal functional activity to temporal RNA expression patterns. The 85 kDa MMP present on gelatin zymography but absent on casein zymography is likely MMP9, while the prominent 20 kDa MMP is most likely MMP3/10b. When purified MMP3/10b

is activated by APMA for 2 h and then incubated at room temperature or 37°C for 1–7 days, several active forms of the protease are generated ranging in size from 20 to 45 kDa (data not shown). However, purified MMP3/10a does not produce an active 20 kDa MMP when processed similarly. This suggests that the 20 kDa MMP present in the regeneration extract is produced either by MMP3/10b self-processing or by cleavage of MMP3/10b with another protease. The 25–60 kDa MMPs present on both gelatin and casein zymography gels are most likely latent or alternatively processed forms of MMP3/10b and MMP3/10a. This interpretation is consistent with previous reports demonstrating that mammalian stromelysins, which can digest both gelatin and casein, exist in several active forms ranging in size from 21 to 45 kDa (Chin et al., 1985; Marcy et al., 1991; Sanchez-Lopez et al., 1988).

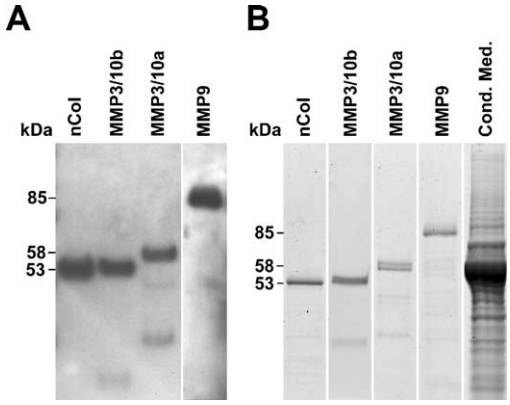


Fig. 4. Purification of newt MMP recombinant proteins. (A) Western blot of affinity-chromatography purified FLAG-tagged nCol, MMP3/10b, MMP3/10a, and MMP9. Anti-FLAG M2 antibody was used as primary antibody and the signals were detected by chemiluminescence. (B) The purified proteins separated by SDS–PAGE and stained with Gelcode Blue (Pierce). A lane containing conditioned medium from HEK 293 cells is shown to illustrate the degree of purification.

### *Spatial expression patterns of MMP genes*

RNA in situ hybridization of fixed tissue sections taken from early limb regenerates revealed the spatial expression patterns of each MMP gene (Fig. 3). The expression of each of these genes can be assigned to cells found in anatomically- or histologically-defined regions of the regenerating limb. From days 1 to 5 postamputation, *nCol* is expressed in bone marrow cells, periosteal cells, and the basal cell layer of the

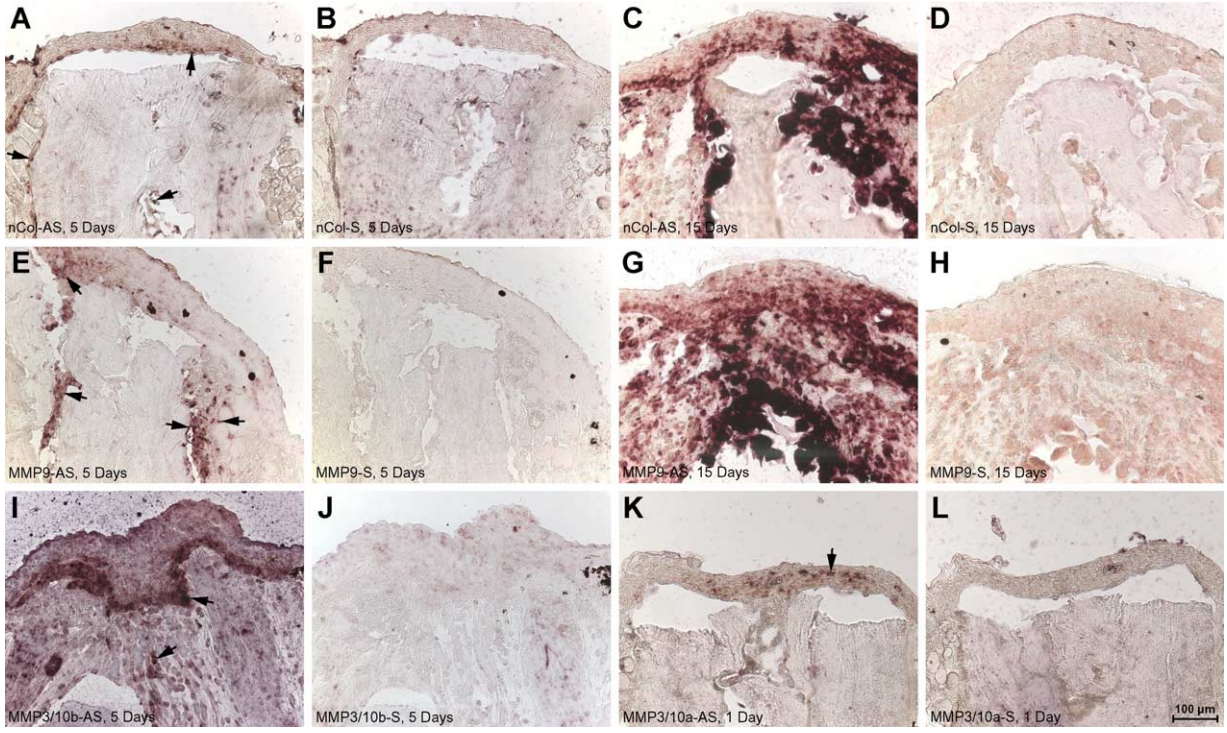


Fig. 3. RNA in situ hybridization of newt limb regenerates. (A and C) *nCol* antisense riboprobe hybridizes to the basal cell layer of the AEC (upper arrow), periosteal cells (left arrow), and bone marrow cells (lower arrow) in a 5-day limb regenerate (A) and expands to include blastemal cells in the 15-day regenerate (C). (E and G) MMP9 antisense riboprobe hybridizes to the basal cell layer of the AEC (upper arrow), bone marrow cells (lower left arrow), periosteal cells, (lower middle arrow), and cells in the region of the dedifferentiating muscle (lower right arrow) in a 5-day limb regenerate (E) and greatly expands to include blastemal cells in the 15-day regenerate (G). (I) MMP3/10b antisense riboprobe hybridizes to the basal cell layer of the AEC (upper arrow) and to internal cells in the region where muscle dedifferentiation is occurring (lower arrow). (K) MMP3/10a antisense riboprobe hybridizes to cells in the wound epithelium (arrow). (B, F, J, and L) Sense riboprobe controls for *nCol*, MMP9, MMP3/10b, and MMP3/10a, respectively, for 1- or 5-day limb regenerates. (D and H) Sense riboprobe controls for *nCol* and MMP9, respectively, for 15-day regenerates. For each gene, matched antisense and sense sections were from the same regenerating limb.

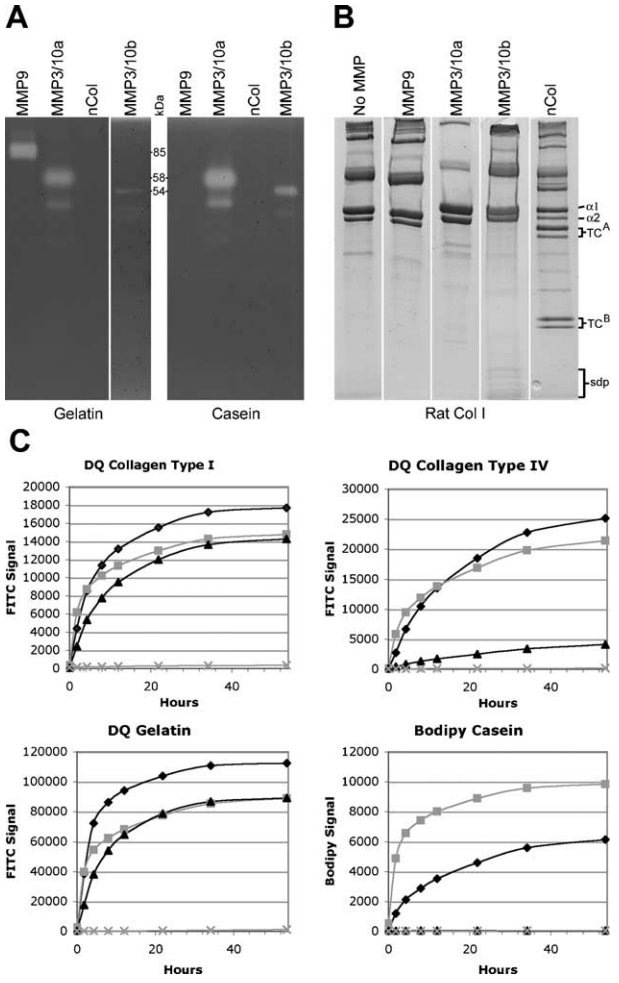


Fig. 5. Biochemical activity of the purified newt MMP proteins. (A) Gelatin and casein zymography. MMP3/10a and MMP3/10b digest both gelatin and casein, MMP9 digests gelatin but not casein, and nCol digests neither substrate. Each lane contains 100 fmol of purified protein. (B) nCol digests rat tail type I collagen (Rat Col I), yielding the characteristic $TC^A$ (3/4) and $TC^B$ (1/4) collagen I fragments following SDS–PAGE. MMP3/10b digests Rat Col I yielding numerous small degradation products (sdp) that are <25 kDa in length. MMP3/10a exhibits little, if any, activity toward Rat Col I, while MMP9 has no activity toward Rat Col I. Two α1 and a single α2 peptide chain comprise the native triple helical form of Rat Col I. (C) The time-dependent dequenching of DQ-Collagen I, DQ-Collagen IV, DQ-gelatin, or BODIPY-casein by digestion of these substrates with activated newt MMPs. Gray x's, nCol activity; gray squares, MMP3/10b activity; black diamonds, MMP3/10a activity; and black triangles, MMP9 activity.

WE/AEC. *MMP3/10b* is expressed throughout the regenerating limb with especially high levels of transcript in the basal cell layer of the WE/AEC, bone marrow cells, and the internal limb cells in the region of muscle dedifferentiation. *MMP3/10a* is expressed only in the WE at day 1, while *MMP9* is expressed in bone marrow cells, the basal layer of the WE/AEC, periosteal cells, and near the region of muscle dedifferentiation. Given that both *nCol* and *MMP9* exhibit bimodal expression patterns, we performed in situ hybridization on limb regenerates during the second wave of expression. At day 15 postamputation, *nCol* and *MMP9* exhibited greatly expanded spatial expression patterns (Figs. 3C, D, G, and H) with both genes being highly expressed in the cells of the blastema, as well as the cells of the AEC, periosteum, and bone marrow.

### *Purified newt MMPs are biochemically functional and exhibit substrate specificity*

Recombinant newt MMPs containing a FLAG-tag on their C-terminal ends were purified by affinity chromatography (Fig. 4). Upon activation with APMA, each of the purified MMP proteins exhibited its own substrate profile when tested using gelatin and casein zymography, a rat tail type I collagen digestion assay, and DQ- and BODIPY-substrate analyses (Figs. 5A–C; Table 1). DQ- and BODIPY-substrates consist of proteins that have been labeled with fluorescent dyes to such a high degree that the fluorescence is quenched by intramolecular interactions between the dye molecules. When the protein is digested by MMPs, the intramolecular quenching ceases and there is a dramatic increase in fluorescence that is proportional to MMP activity. By using the above assays, we showed that nCol readily digested native rat tail type I collagen to produce the typical $TC^A$ (3/4) and $TC^B$ (1/4) collagen fragments but failed to digest gelatin, casein, collagen IV, or a processed form of collagen I. These results confirm that nCol is a true collagenase, but unlike *Xenopus* MMP18, its closest relative, it does not digest gelatin (Stolow et al., 1996). MMP3/10b readily digested gelatin, casein, collagen IV, and processed collagen I, and exhibited an atypical activity toward native rat tail type I collagen by generating several small collagen degradation products with sizes <25 kDa (Fig. 5B). Therefore, MMP3/10b acts both as a stromelysin and noncanonical collagenase. MMP3/10a digested gelatin, casein, collagen IV, and processed collagen I; however, it exhibited little, if any, activity toward native rat tail type I collagen. Newt MMP9 digested gelatin, collagen IV, processed collagen I, but not casein and native rat tail type I collagen.

### *Treatment of regenerating newt limbs with GM6001 leads to aberrant limb regenerates*

All purified newt MMPs and MMPs identified in the newt extracts were completely inhibited by 50 μM

Table 1
Substrate specificities for newt MMPs

| Protease | Native type I collagen | Processed collagen I | Collagen IV | Gelatin | Casein |
|---|---|---|---|---|---|
| nCol | +++ | – | – | – | – |
| MMP3/10b | +++ | +++ | +++ | +++ | +++ |
| MMP3/10a | – | +++ | +++ | +++ | +++ |
| MMP9 | – | +++ | ++ | +++ | – |

Number of +'s represents relative strength of substrate cleavage; –, no activity observed.

GM6001, except for some residual activity of the 20 kDa MMP (Fig. 6). However, this residual activity, presumably due to a processed form of MMP3/10b (see above), was less than the activity observed in unamputated newt limbs. To determine whether MMPs might be required for normal limb regeneration, we amputated newt forelimbs through the stylopodium midway between the shoulder and elbow and within an hour of amputation placed the newts in dechlorinated tap water containing 50 μM GM6001 and 1% DMSO. The DMSO was present for two reasons: (1) it is a preferred solvent for GM6001 and (2) it is thought to allow passage of GM6001 through the extracellular spaces between epithelial cells (Zhang and Sarras, 1994). Newts were housed continually in the GM6001/DMSO solution for 60 days while their limbs regenerated. Control newts were placed in 1% DMSO or dechlorinated tap water for the entire regenerative period. Following regeneration, the limbs were examined for general morphological and histological abnormalities. All 10 GM6001-treated limbs exhibited abnormalities, while the 6 DMSO-treated limbs and all water control limbs exhibited normal regenerative morphology. Using the

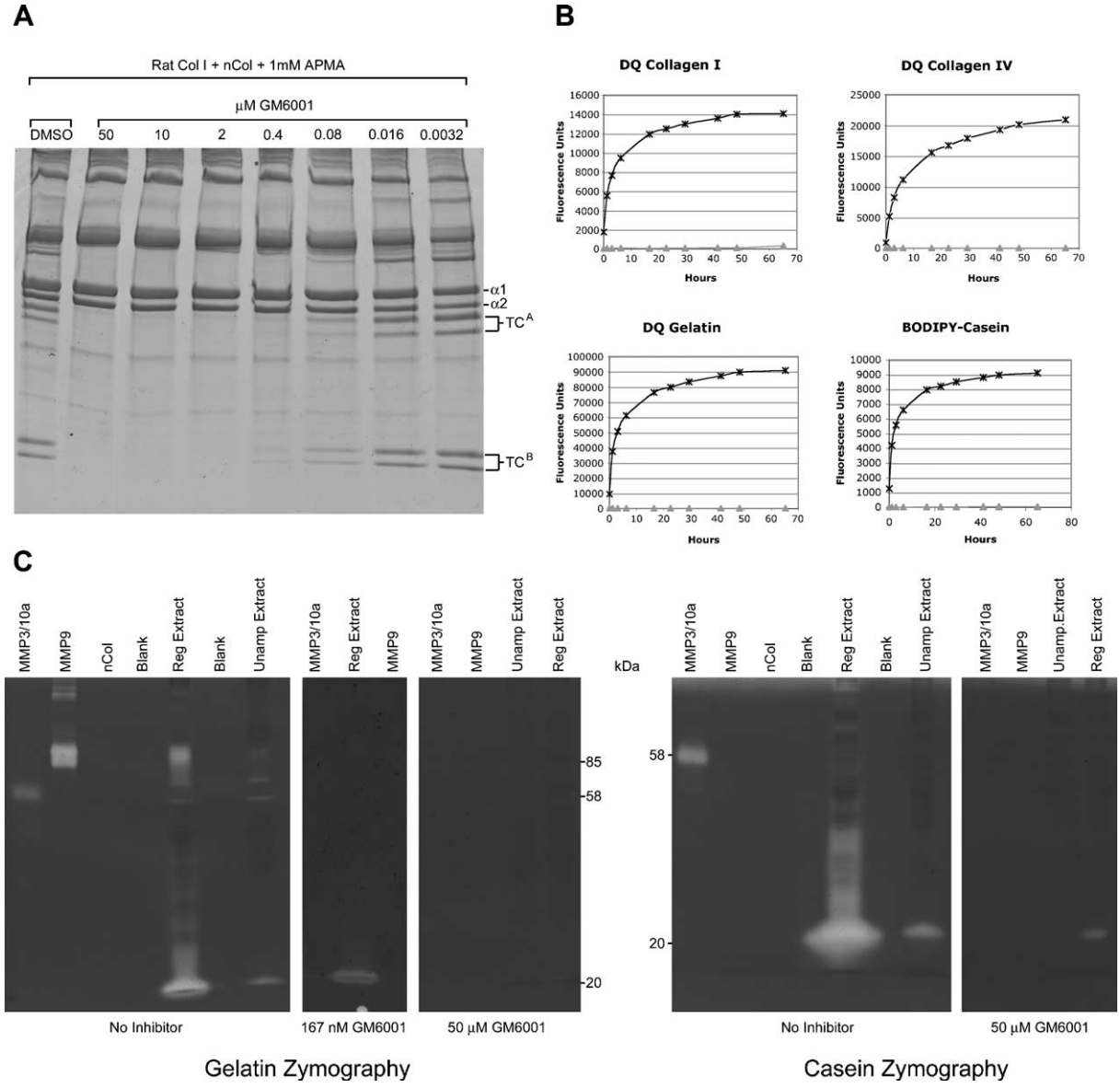


Fig. 6. GM6001 inhibits newt MMP proteolytic activity. (A) GM6001 inhibits nCol activity. At concentrations ≥2 μM, GM6001 completely inhibits the nCol-mediated cleavage of native rat tail type I collagen (Rat Col I) to form the $TC^A$ and $TC^B$ fragments. 1% DMSO does not inhibit nCol activity. (B) At concentrations of 2 μM, GM6001 inhibits MMP3/10b against all tested substrates. Black asterisks represent the activity of uninhibited MMP3/10b against each substrate. Gray triangles represent the activity of MMP3/10b against each substrate in the presence of 2 μM GM6001. (C) GM6001 inhibits MMP3/10a, MMP9, and all MMPs found in the regenerating newt limb that cleave gelatin and/or casein during gel zymography. Residual activity of the 20 kDa MMP, presumably a processed form of MMP3/10b, remains even at 50 μM GM6001; however, this activity is below that observed in unamputated newt limbs.

Fischer–Irwin exact test, the difference in outcome between GM6001- and DMSO-treated limbs is statistically significant at $P = 0.0001$.

Most of the GM6001-treated limbs (8 out of 10) were dwarfed and appeared inflexible at the elbow. Hematoxylin- and eosin-stained sections of these limbs also revealed abnormalities (Fig. 7). The dwarfed limbs had shorter regenerated humeri, ulnae, and radii than their control counterparts (Figs. 7B and C; Table 2). In addition, each of the regenerated humeri in GM6001-treated limbs lacked a well-formed, rounded distal epiphysis, which resulted in an aberrant articulation with the radius and ulna. This aberrant joint most likely explains the observation that the GM6001-treated limbs appeared to be inflexible at the elbow. Limbs from control newts did not exhibit these abnormalities. The regenerated portion of the humeri in GM6001-treated limbs was, on average, 48% the length of regenerated control humeri, while the regenerated ulnae and radii of treated newts were 52% and 53% the length of their corresponding DMSO controls, respectively (Table 2). These differences in mean length are statistically significant. No statistically significant differences in the widths of the regenerated bones are observed. In 2 out of 10 limbs, regeneration was halted at an early stage and only a healed stump was observed (Fig. 7D). Histological analysis revealed that the distal end of these stumps was covered by an uncharacterized acellular scar-like substance.

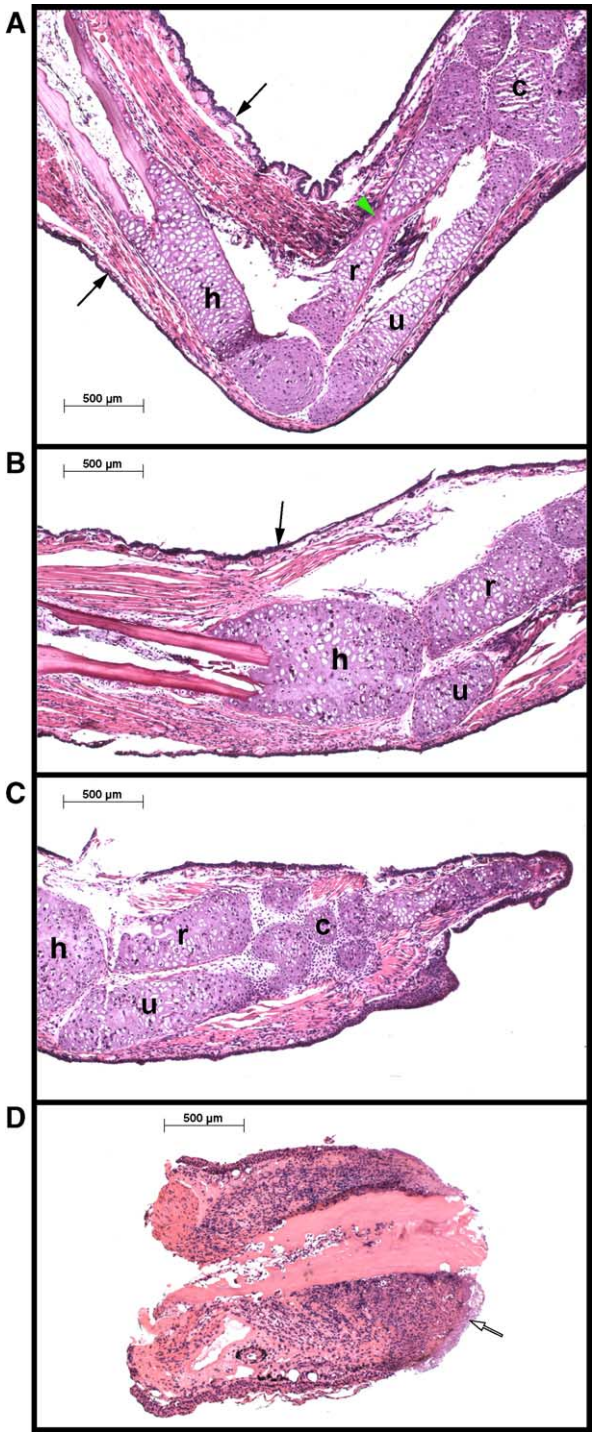


## Discussion

Our results strongly suggest that MMPs are required for normal newt limb regeneration. First, all newts treated with the MMP inhibitor GM6001 either failed to regenerate their limbs or regenerated abnormal limbs, while newts treated with the vehicle alone exhibited no impairment in regeneration. GM6001 is a potent inhibitor of metalloproteases that has been used extensively to inhibit MMP proteolytic activity both in vitro and in vivo (Alexander et al., 1996; Gijbels et al., 1994; Grobelny et al., 1992; Kheradmand et al., 2002; Leontovich et al., 2000; Solberg et al., 2003; Wiseman et al., 2003). Second, MMP expression and activity are highly elevated within hours of limb amputation, suggesting that these proteases play an important role in the initial stages of limb regeneration. Third, the expression of *MMP3/10b*, *nCol*, and *MMP9* in tissues undergoing histolysis (Fig. 3) suggests that these MMPs contribute to the histolytic process during regeneration.

Fig. 7. Inhibition of MMP proteolytic activity by GM6001 during newt limb regeneration produces dwarfed and malformed limbs. (A) Section of the stylopodium and zeugopodium of a regenerated control limb treated with 1% DMSO throughout the 60-day regenerative period. Note that ossification of the regenerated radius is beginning in the diaphysis as described previously (Stock et al., 2003) (green arrowhead). (B) Section of the stylopodium and zeugopodium of a regenerated limb treated with 50 μM GM6001 throughout the 60-day regenerative period. (C) Section of the zeugopodium and autopodium of a regenerated limb treated with 50 μM GM6001 throughout the 60-day regenerative period. (D) Section of a limb treated with 50 μM GM6001 for 60 days that failed to regenerate. Note the acellular scar-like substance at the distal end of the limb stump (white arrow). Black arrows denote approximate amputation plane. h, regenerated humerus; r, regenerated radius; u, regenerated ulna; c, regenerated carpal bone.

Table 2
Inhibitory effects of GM6001 on newt limb regeneration

| Treatment | Regenerated humerus[a] | | Regenerated ulna[a] | | Regenerated radius[a] | |
|---|---|---|---|---|---|---|
| | Length (μm) | Width (μm) | Length (μm) | Width (μm) | Length (μm) | Width (μm) |
| DMSO | 1408 ± 82 | 578 ± 122 | 1702 ± 339 | 308 ± 73 | 1646 ± 308 | 375 ± 50 |
| GM6001 | 671 ± 156 | 665 ± 85 | 881 ± 359 | 384 ± 107 | 869 ± 331 | 406 ± 132 |
| *P* value | $4.1 \times 10^{-8}$[b] | $8.1 \times 10^{-2}$ | $8.1 \times 10^{-4}$[b] | $7.7 \times 10^{-2}$ | $6.2 \times 10^{-4}$[b] | $2.8 \times 10^{-1}$ |

[a] Measurements are given as the mean ± the standard deviation.
[b] Statistically significant results between the DMSO control and GM6001-treated limbs.

Eight of the ten limbs treated with the MMP inhibitor were hypomorphic and malformed. This phenotype is consistent with other studies that have addressed the role of MMPs during mouse development or regeneration in less complex organisms. In our study, the regenerated humeri, radii, and ulnae of newts treated with GM6001 were about 50% the length of the corresponding control bones. In comparison, mice that are deficient for MMP14 develop dwarfed limbs that are about 65% the length of their wild type littermates (Holmbeck et al., 1999). Hydra foot regeneration (Leontovich et al., 2000) and intestinal regeneration in the sea cucumber *Holothuria glaberrima* (Quinones et al., 2002) are impaired by MMP inhibition. These similarities in response to MMP deficiency or inhibition suggest that MMPs play important roles in the development and regeneration of complex structures. Expression studies of MMPs during salamander spinal cord regeneration (Chernoff et al., 2000) and ear hole regeneration in MRL mice (Gourevitch et al., 2003) are consistent with this interpretation.

It is reasonable to propose that MMPs might be involved in the formation, maintenance, and growth of the regeneration blastema, given that they are initially expressed in tissues that contribute to blastema formation and then later in the blastema itself (see Fig. 3). For example, the bimodal expression patterns of *nCol* and *MMP9* suggest that these two MMPs each have dual roles during regeneration, one very early in the process when cells are receiving the initial dedifferentiation signals and the other several days later during the stage of blastemal growth. *MMP9* exhibits a similar bimodal expression pattern during limb regeneration in the axolotl *Ambystoma mexicanum* (Yang et al., 1999), providing further evidence for a potential dual role for this MMP. Our in situ hybridization data are consistent with such an interpretation. During the first few days of regeneration, *nCol* and *MMP9* are expressed in periosteal and/or muscle cells, which dedifferentiate and contribute to the formation of the blastema (Hay and Fischman, 1961). During the second wave of expression, both *nCol* and *MMP9* have greatly expanded their expression domains to include blastemal cells, suggesting that these genes are also important for blastemal growth or maintenance. The expression of *MMP3/10b* in tissues that are about to undergo dedifferentiation further strengthens our hypothesis. It has been shown that MMP3, a mammalian stromelysin related to newt MMP3/10b, can promote the spontaneous development of hyperplasia, dysplasia, and carcinoma in mammary glands of transgenic mice (Sternlicht et al., 1999, 2000). This suggests that stromelysins, such as MMP3/10b, could act to promote cell transformation and proliferation, which are events similar to those occurring during the dedifferentiation and blastemal stages of limb regeneration. *MMP3/10b* has the highest upregulation of the MMP genes and likely encodes the prominent 20 kDa MMP present in early limb regenerates. MMP3/10b also exhibits an unusual set of proteolytic activities (see Fig. 5), which could be the reason for its apparent importance during limb regeneration. The two phenotypes we observed in our MMP inhibitor studies are also consistent with the hypothesis that MMPs are involved in blastema formation, maintenance, and growth. Reduced blastema size due to insufficient cellular dedifferentiation or proliferation could explain both the presence of limb stumps and the development of dwarfed limbs following MMP inhibition.

MMPs could exert their effects on regeneration by preventing scar formation while promoting the production of an ECM that is conducive to blastema formation and growth. This interpretation is consistent with our data. Two of the GM6001-treated limbs completely failed to regenerate and instead formed an acellular scar-like structure on the distal end of the limb stump. This possible mechanism of MMP function was first proposed by Grillo et al. (1968), and since that time, ample evidence has been generated that suggests there is an antithetical relationship between scar formation and regeneration. Midgestational fetal mammalian skin can regenerate perfectly following an incisional wound, while postnatal and adult skin respond to similar wounds by forming a scar (Bullard et al., 1997; Colwell et al., 2003; Lovvorn et al., 1999). When fetal skin is injected with TGFβ1, MMP1 levels are reduced and scars are formed (Bullard et al., 1997), suggesting that high MMP levels may prevent scar formation during fetal skin regeneration. Furthermore, zebrafish normally regenerate their heart ventricles following the apical excision of 20–30% of the ventricle (Poss et al., 2002; Raya et al., 2003); however, a mutation in an essential regeneration gene leads to scar formation instead of regeneration (Poss et al., 2002). Given the antithetical relationship between regeneration and scar formation and the known biochemical functions of MMPs, it is not surprising that MMPs might

function to prevent scar formation while promoting an ECM conducive to regeneration.

MMPs could exert their biological functions during regeneration through a variety of mechanisms. As mentioned above, they could influence blastemal formation by selectively degrading components of the ECM. Alternatively, they are known to be involved in several biological activities including the activation of latent MMPs (Sternlicht and Werb, 2001; Strongin et al., 1995), cytokines (Schonbeck et al., 1998; Yu and Stamenkovic, 2000), and small biopeptides (Dong et al., 1997; Patterson and Sang, 1997), the release of trapped growth factors bound to either the ECM or non-matrix proteins (Fowlkes et al., 1994a,b, 1995; Imai et al., 1997; Thrailkill et al., 1995; Whitelock et al., 1996), the cleavage of cell surface proteins (Haro et al., 2000; Kayagaki et al., 1995; Levi et al., 1996; Noe et al., 2001; Sheu et al., 2001), and the initiation of intracellular signaling pathways (Conant et al., 2002; Galt et al., 2002). Any or all of these biological functions could be required for the formation, growth, and maintenance of the regeneration blastema.

In summary, MMPs appear to be required for normal regeneration in a variety of organisms including newts, hydra, and sea cucumbers. This convergence on a set of required regeneration genes in three species, each representing a different phylum, suggests that there may be a common set of molecular factors and pathways that govern most regenerative processes. If so, it will be important to study regeneration in a wide variety of organisms, so that these common molecular pathways can be identified. Such knowledge will lead to a better understanding of the molecular basis for regeneration and may foster rational therapies for regenerative medicine.

## Acknowledgments

We thank Alejandro Sanchez Alvarado, Tom McIntyre, Ken Poss, Andrew Weyrich, and Ivor Benjamin for helpful suggestions. We also thank Tom McIntyre, Brenda Bass, and Dean Li for allowing us generous use of the Perkin-Elmer Fusion α microplate reader, the Molecular Dynamics Storm 860, and histology equipment, respectively. This work was supported by NIH grant number R01 NS43878 to SJO and an HHMI Medical Student Fellowship to VV.

## References

Alexander, C.M., Howard, E.W., Bissell, M.J., Werb, Z., 1996. Rescue of mammary epithelial cell apoptosis and entactin degradation by a tissue inhibitor of metalloproteinases-1 transgene. J. Cell Biol. 135, 1669–1677.

Bodemer, C.W., Everett, N.B., 1959. Localization of newly synthesized proteins in regenerating newt limbs as determined by radioautographic localization of injected methionine-S35. Dev. Biol. 1, 327–342.

Brockes, J.P., Kumar, A., 2002. Plasticity and reprogramming of differentiated cells in amphibian regeneration. Nat. Rev. Mol. Cell Biol. 3, 566–574.

Bullard, K.M., Cass, D.L., Banda, M.J., Adzick, N.S., 1997. Transforming growth factor beta-1 decreases interstitial collagenase in healing human fetal skin. J. Pediatr. Surg. 32, 1023–1027.

Butler, E.G., Ward, M.B., 1967. Reconstitution of the spinal cord after ablation in adult Triturus. Dev. Biol. 15, 464–486.

Chalkley, D.T., 1954. A quantitative histological analysis of forelimb regeneration in *Triturus viridescens*. J. Morphol. 94, 21–70.

Chernoff, E.A., O'Hara, C.M., Bauerle, D., Bowling, M., 2000. Matrix metalloproteinase production in regenerating axolotl spinal cord. Wound Repair Regen. 8, 282–291.

Chin, J.R., Murphy, G., Werb, Z., 1985. Stromelysin, a connective tissue-degrading metalloendopeptidase secreted by stimulated rabbit synovial fibroblasts in parallel with collagenase. Biosynthesis, isolation, characterization, and substrates. J. Biol. Chem. 260, 12367–12376.

Colwell, A.S., Longaker, M.T., Lorenz, H.P., 2003. Fetal wound healing. Front. Biosci. 8, s1240–s1248.

Conant, K., Haughey, N., Nath, A., St Hillaire, C., Gary, D.S., Pardo, C.A., Wahl, L.M., Bilak, M., Milward, E., Mattson, M.P., 2002. Matrix metalloproteinase-1 activates a pertussis toxin-sensitive signaling pathway that stimulates the release of matrix metalloproteinase-9. J. Neurochem. 82, 885–893.

Dong, Z., Kumar, R., Yang, X., Fidler, I.J., 1997. Macrophage-derived metalloelastase is responsible for the generation of angiostatin in Lewis lung carcinoma. Cell 88, 801–810.

Fowlkes, J.L., Enghild, J.J., Suzuki, K., Nagase, H., 1994a. Matrix metalloproteinases degrade insulin-like growth factor-binding protein-3 in dermal fibroblast cultures. J. Biol. Chem. 269, 25742–25746.

Fowlkes, J.L., Suzuki, K., Nagase, H., Thrailkill, K.M., 1994b. Proteolysis of insulin-like growth factor binding protein-3 during rat pregnancy: a role for matrix metalloproteinases. Endocrinology 135, 2810–2813.

Fowlkes, J.L., Thrailkill, K.M., Serra, D.M., Suzuki, K., Nagase, H., 1995. Matrix metalloproteinases as insulin-like growth factor binding protein-degrading proteinases. Prog. Growth Factor Res. 6, 255–263.

Galt, S.W., Lindemann, S., Allen, L., Medd, D.J., Falk, J.M., McIntyre, T.M., Prescott, S.M., Kraiss, L.W., Zimmerman, G.A., Weyrich, A.S., 2002. Outside-in signals delivered by matrix metalloproteinase-1 regulate platelet function. Circ. Res. 90, 1093–1099.

Gijbels, K., Galardy, R.E., Steinman, L., 1994. Reversal of experimental autoimmune encephalomyelitis with a hydroxamate inhibitor of matrix metalloproteases. J. Clin. Invest. 94, 2177–2182.

Gourevitch, D., Clark, L., Chen, P., Seitz, A., Samulewicz, S.J., Heber-Katz, E., 2003. Matrix metalloproteinase activity correlates with blastema formation in the regenerating MRL mouse ear hole model. Dev. Dyn. 226, 377–387.

Grillo, H.C., Lapiere, C.M., Dresden, M.H., Gross, J., 1968. Collagenolytic activity in regenerating forelimbs of the adult newt (*Triturus viridescens*). Dev. Biol. 17, 571–583.

Grobelny, D., Poncz, L., Galardy, R.E., 1992. Inhibition of human skin fibroblast collagenase, thermolysin, and Pseudomonas aeruginosa elastase by peptide hydroxamic acids. Biochemistry 31, 7152–7154.

Gross, J., Lapiere, C.M., 1962. Collagenolytic activity in amphibian tissues: a tissue culture assay. Proc. Natl. Acad. Sci. U. S. A. 48, 1014–1022.

Haro, H., Crawford, H.C., Fingleton, B., Shinomiya, K., Spengler, D.M., Matrisian, L.M., 2000. Matrix metalloproteinase-7-dependent release of tumor necrosis factor-alpha in a model of herniated disc resorption. J. Clin. Invest. 105, 143–150.

Hay, E.D., Fischman, D.A., 1961. Origin of the blastema in regenerating limbs of the newt *Triturus viridescens*. An autoradiographic study using tritiated thymidine to follow cell proliferation and migration. Dev. Biol. 3, 26–59.

Holmbeck, K., Bianco, P., Caterina, J., Yamada, S., Kromer, M., Kuznetsov, S.A., Mankani, M., Robey, P.G., Poole, A.R., Pidoux, I., Ward, J.M., Birkedal-Hansen, H., 1999. MT1-MMP-deficient mice develop dwarfism, osteopenia, arthritis, and connective tissue disease due to inadequate collagen turnover. Cell 99, 81–92.

Imai, K., Hiramatsu, A., Fukushima, D., Pierschbacher, M.D., Okada, Y., 1997. Degradation of decorin by matrix metalloproteinases: identifica-

tion of the cleavage sites, kinetic analyses and transforming growth factor-beta1 release. Biochem. J. 322 (Pt. 3), 809–814.
Kato, T., Miyazaki, K., Shimizu-Nishikawa, K., Koshiba, K., Obara, M., Mishima, H.K., Yoshizato, K., 2003. Unique expression patterns of matrix metalloproteinases in regenerating newt limbs. Dev. Dyn. 226, 366–376.
Kayagaki, N., Kawasaki, A., Ebata, T., Ohmoto, H., Ikeda, S., Inoue, S., Yoshino, K., Okumura, K., Yagita, H., 1995. Metalloproteinase-mediated release of human Fas ligand. J. Exp. Med. 182, 1777–1783.
Kheradmand, F., Rishi, K., Werb, Z., 2002. Signaling through the EGF receptor controls lung morphogenesis in part by regulating MT1-MMP-mediated activation of gelatinase A/MMP2. J. Cell Sci. 115, 839–848.
Leontovich, A.A., Zhang, J., Shimokawa, K., Nagase, H., Sarras Jr., M.P., 2000. A novel hydra matrix metalloproteinase (HMMP) functions in extracellular matrix degradation, morphogenesis and the maintenance of differentiated cells in the foot process. Development 127, 907–920.
Levi, E., Fridman, R., Miao, H.Q., Ma, Y.S., Yayon, A., Vlodavsky, I., 1996. Matrix metalloproteinase 2 releases active soluble ectodomain of fibroblast growth factor receptor 1. Proc. Natl. Acad. Sci. U. S. A. 93, 7069–7074.
Lovvorn III, H.N., Cheung, D.T., Nimni, M.E., Perelman, N., Estes, J.M., Adzick, N.S., 1999. Relative distribution and crosslinking of collagen distinguish fetal from adult sheep wound repair. J. Pediatr. Surg. 34, 218–223.
Marcy, A.I., Eiberger, L.L., Harrison, R., Chan, H.K., Hutchinson, N.I., Hagmann, W.K., Cameron, P.M., Boulton, D.A., Hermes, J.D., 1991. Human fibroblast stromelysin catalytic domain: expression, purification, and characterization of a C-terminally truncated form. Biochemistry 30, 6476–6483.
McGann, C.J., Odelberg, S.J., Keating, M.T., 2001. Mammalian myotube dedifferentiation induced by newt regeneration extract. Proc. Natl. Acad. Sci. U. S. A. 98, 13699–13704.
Mescher, A.L., 1976. Effects on adult newt limb regeneration of partial and complete skin flaps over the amputation surface. J. Exp. Zool. 195, 117–128.
Miyazaki, K., Uchiyama, K., Imokawa, Y., Yoshizato, K., 1996. Cloning and characterization of cDNAs for matrix metalloproteinases of regenerating newt limbs. Proc. Natl. Acad. Sci. U. S. A. 93, 6819–6824.
Noe, V., Fingleton, B., Jacobs, K., Crawford, H.C., Vermeulen, S., Steelant, W., Bruyneel, E., Matrisian, L.M., Mareel, M., 2001. Release of an invasion promoter E-cadherin fragment by matrilysin and stromelysin-1. J. Cell Sci. 114, 111–118.
Park, I.S., Kim, W.S., 1999. Modulation of gelatinase activity correlates with the dedifferentiation profile of regenerating salamander limbs. Mol. Cells 9, 119–126.
Patterson, B.C., Sang, Q.A., 1997. Angiostatin-converting enzyme activities of human matrilysin (MMP-7) and gelatinase B/type IV collagenase (MMP-9). J. Biol. Chem. 272, 28823–28825.
Poss, K.D., Wilson, L.G., Keating, M.T., 2002. Heart regeneration in zebrafish. Science 298, 2188–2190.
Quinones, J.L., Rosa, R., Ruiz, D.L., Garcia-Arraras, J.E., 2002. Extracellular matrix remodeling and metalloproteinase involvement during intestine regeneration in the sea cucumber *Holothuria glaberrima*. Dev. Biol. 250, 181–197.
Raya, A., Koth, C.M., Buscher, D., Kawakami, Y., Itoh, T., Raya, R.M., Sternik, G., Tsai, H.J., Rodriguez-Esteban, C., Izpisua-Belmonte, J.C., 2003. Activation of Notch signaling pathway precedes heart regeneration in zebrafish. Proc. Natl. Acad. Sci. U. S. A. 100 (Suppl. 1), 11889–11895.
Sanchez-Lopez, R., Nicholson, R., Gesnel, M.C., Matrisian, L.M., Breathnach, R., 1988. Structure–function relationships in the collagenase family member transin. J. Biol. Chem. 263, 11892–11899.
Schonbeck, U., Mach, F., Libby, P., 1998. Generation of biologically active IL-1 beta by matrix metalloproteinases: a novel caspase-1-independent pathway of IL-1 beta processing. J. Immunol. 161, 3340–3346.
Sheu, B.C., Hsu, S.M., Ho, H.N., Lien, H.C., Huang, S.C., Lin, R.H., 2001. A novel role of metalloproteinase in cancer-mediated immunosuppression. Cancer Res. 61, 237–242.
Solberg, H., Rinkenberger, J., Dano, K., Werb, Z., Lund, L.R., 2003. A functional overlap of plasminogen and MMPs regulates vascularization during placental development. Development 130, 4439–4450.
Sternlicht, M.D., Werb, Z., 2001. How matrix metalloproteinases regulate cell behavior. Annu. Rev. Cell Dev. Biol. 17, 463–516.
Sternlicht, M.D., Lochter, A., Sympson, C.J., Huey, B., Rougier, J.P., Gray, J.W., Pinkel, D., Bissell, M.J., Werb, Z., 1999. The stromal proteinase MMP3/stromelysin-1 promotes mammary carcinogenesis. Cell 98, 137–146.
Sternlicht, M.D., Bissell, M.J., Werb, Z., 2000. The matrix metalloproteinase stromelysin-1 acts as a natural mammary tumor promoter. Oncogene 19, 1102–1113.
Stock, S.R., Blackburn, D., Gradassi, M., Simon, H.G., 2003. Bone formation during forelimb regeneration: a microtomography (microCT) analysis. Dev. Dyn. 226, 410–417.
Stolow, M.A., Bauzon, D.D., Li, J., Sedgwick, T., Liang, V.C., Sang, Q.A., Shi, Y.B., 1996. Identification and characterization of a novel collagenase in *Xenopus laevis*: possible roles during frog development. Mol. Biol. Cell 7, 1471–1483.
Strongin, A.Y., Collier, I., Bannikov, G., Marmer, B.L., Grant, G.A., Goldberg, G.I., 1995. Mechanism of cell surface activation of 72-kDa type IV collagenase. Isolation of the activated form of the membrane metalloprotease. J. Biol. Chem. 270, 5331–5338.
Tatusova, T.A., Madden, T.L., 1999. BLAST 2 sequences, a new tool for comparing protein and nucleotide sequences. FEMS Microbiol. Lett. 174, 247–250.
Thompson, J.D., Higgins, D.G., Gibson, T.J., 1994. CLUSTAL W: improving the sensitivity of progressive multiple sequence alignment through sequence weighting, position-specific gap penalties and weight matrix choice. Nucleic Acids Res. 22, 4673–4680.
Thornton, C.S., 1957. The effects of apical cap removal on limb regeneration in *Amblystoma lavae*. J. Exp. Zool. 134, 357–382.
Thornton, C.S., Thornton, M.T., 1965. The regeneration of accessory limb parts following epidermal cap transplantation in urodeles. Experentia 21, 146–151.
Thrailkill, K.M., Quarles, L.D., Nagase, H., Suzuki, K., Serra, D.M., Fowlkes, J.L., 1995. Characterization of insulin-like growth factor-binding protein 5-degrading proteases produced throughout murine osteoblast differentiation. Endocrinology 136, 3527–3533.
Wallace, H., 1981. Vertebrate limb regeneration. John Wiley & Sons, New York.
Whitelock, J.M., Murdoch, A.D., Iozzo, R.V., Underwood, P.A., 1996. The degradation of human endothelial cell-derived perlecan and release of bound basic fibroblast growth factor by stromelysin, collagenase, plasmin, and heparanases. J. Biol. Chem. 271, 10079–10086.
Wiseman, B.S., Sternlicht, M.D., Lund, L.R., Alexander, C.M., Mott, J., Bissell, M.J., Soloway, P., Itohara, S., Werb, Z., 2003. Site-specific inductive and inhibitory activities of MMP-2 and MMP-3 orchestrate mammary gland branching morphogenesis. J. Cell Biol. 162, 1123–1133.
Yang, E.V., Bryant, S.V., 1994. Developmental regulation of a matrix metalloproteinase during regeneration of axolotl appendages. Dev. Biol. 166, 696–703.
Yang, E.V., Gardiner, D.M., Carlson, M.R., Nugas, C.A., Bryant, S.V., 1999. Expression of Mmp-9 and related matrix metalloproteinase genes during axolotl limb regeneration. Dev. Dyn. 216, 2–9.
Yu, Q., Stamenkovic, I., 2000. Cell surface-localized matrix metalloproteinase-9 proteolytically activates TGF-beta and promotes tumor invasion and angiogenesis. Genes Dev. 14, 163–176.
Zhang, X., Sarras Jr., M.P., 1994. Cell-extracellular matrix interactions under in vivo conditions during interstitial cell migration in Hydra vulgaris. Development 120, 425–432.